Aluminum inhibits the plasma membrane and sarcoplasmic reticulum Ca2+-ATPases by different mechanisms

Marilina de Sautu, Nicolás A. Saffioti, Mariela S. Ferreira-Gomes, Rolando C. Rossi, Juan Pablo F.C. Rossi, Irene C. Mangialavori

PII: S0005-2736(18)30156-1
DOI: doi:10.1016/j.bbamem.2018.05.014
Reference: BBAMEM 82785

To appear in: *BBA - Biomembranes*

Received date: 25 January 2018
Revised date: 28 April 2018
Accepted date: 25 May 2018

Please cite this article as: Marilina de Sautu, Nicolás A. Saffioti, Mariela S. Ferreira-Gomes, Rolando C. Rossi, Juan Pablo F.C. Rossi, Irene C. Mangialavori , Aluminum inhibits the plasma membrane and sarcoplasmic reticulum Ca2+-ATPases by different mechanisms. Bbamem (2018), doi:10.1016/j.bbamem.2018.05.014

Aluminum Inhibits the Plasma Membrane and Sarcoplasmic Reticulum Ca^{2+}-ATPases by Different Mechanisms

Marilina de Sautu[§], Nicolás A. Saffioti[§], Mariela S. Ferreira-Gomes, Rolando C. Rossi, Juan Pablo F. C. Rossi and Irene C. Mangialavori[#]

[§]Both authors contributed equally to this work

From Universidad de Buenos Aires, Consejo Nacional de Investigaciones Científicas y Técnicas (CONICET), Instituto de Química y Fisicoquímica Biológicas (IQUIFIB), Facultad de Farmacia y Bioquímica, Junín 956, Ciudad Autónoma de Buenos Aires C1113AAD, Argentina.

Running title: *Aluminum inhibits distinctly PMCA and SERCA*

[#]To whom correspondence should be addressed: Irene Mangialavori, Instituto de Química y Fisicoquímica Biológicas, Facultad de Farmacia y Bioquímica, Universidad de Buenos Aires, CONICET, Junín 956 (1113) Buenos Aires, Argentina. *email*: irenem@qb.ffyb.uba.ar

Keywords: Calcium ATPase, Inhibition mechanism, Phosphorylated intermediate, Calcium, Magnesium, Aluminum, Proteolysis**.**

ABSTRACT

Aluminum (Al^{3+}) is involved in the pathophysiology of neurodegenerative disorders. The mechanisms that have been proposed to explain the action of Al^{3+} toxicity are linked to changes in the cellular calcium homeostasis, placing the transporting calcium pumps as potential targets.

The aim of this work was to study the molecular inhibitory mechanism of Al^{3+} on Ca^{2+}-ATPases such as the plasma membrane and the sarcoplasmic reticulum calcium pumps (PMCA and SERCA, respectively). These P-ATPases transport Ca^{2+} actively from the cytoplasm towards the extracellular medium and to the sarcoplasmic reticulum, respectively. For this purpose, we performed enzymatic measurements of the effect of Al^{3+} on purified preparations of PMCA and SERCA.

Our results show that Al^{3+} is an irreversible inhibitor of PMCA and a slowly-reversible inhibitor of SERCA. The binding of Al^{3+} is affected by Ca^{2+} in SERCA, though not in PMCA. Al^{3+} prevents the phosphorylation of SERCA and, conversely, the dephosphorylation of PMCA. The dephosphorylation time courses of the complex formed by PMCA and Al^{3+} (*E*PAl) in the presence of ADP or ATP show that *E*PAl is composed mainly by the conformer E_2P.

This work shows for the first time a distinct mechanism of Al^{3+} inhibition that involves different intermediates of the reaction cycle of these two Ca^{2+}-ATPases.

Aluminum is one of the most abundant elements in the Earth's crust. The relationship between aluminum exposure and neurodegenerative diseases, including dialysis encephalopathy syndrome, amyotrophic lateral sclerosis, Parkinsonism dementia and Alzheimer's disease has been extensively reported (1). The oxidation state of aluminum is +3, and its effective ionic radius in sixfold coordination is 0.54 Å. The primary interaction of Al^{3+} with ligands is electrostatic and has a slow dissociation rate (2). In aqueous solution, aluminum is solvated with water molecules. This form is known as free aluminum ($Al(H_2O)_6^{3+}$ (or simply, Al^{3+}) and is abundant at acidic pH. When the pH rises, aluminum is complexed with OH^- from deprotonation of water molecules ($Al(OH)_n$). Among others, Al^{3+} binds strongly to ATP and phosphate groups and displaces both Mg^{2+} and Ca^{2+} from their enzyme's binding sites (1). Hence, changes in the Ca^{2+} homeostasis and protein phosphorylation/dephosphorylation would explain aluminum cellular toxicity (2).

Among the most important Ca^{2+} regulatory mechanisms are the Plasma Membrane Calcium ATPase (PMCA) and Sarcoplasmic Reticulum Calcium ATPase (SERCA). These pumps belong to the family of P-ATPases, which share the formation of an acid-stable phosphorylated intermediate as part of their reaction cycle. PMCA and SERCA use the ATP hydrolysis as a source of energy to transport calcium from cytoplasm to the extracellular medium or the reticulum lumen, respectively.

PMCA is more regulated than SERCA, and through its interaction with regulatory, targeting and signaling proteins, regulates both global Ca^{2+} homeostasis and spatially defined Ca^{2+} signaling (3).

Detailed structural information about PMCA is currently lacking. Its little abundance (approximately 0.1% of the total protein in the membrane) and the presence of several isoforms hindered efforts to produce suitable crystals for X-ray diffraction. Although PMCA has not been crystallized yet, the structures of several reaction intermediates of SERCA have been resolved (*For revision, see* 4). Its membrane-buried region is made up of 10 membrane spanning helices and is connected to a large cytoplasmic headpiece, which is further separated into three distinct domains, denoted A ("actuator"), P ("phosphorylation"), and N ("nucleotide binding"). However, unlike SERCA, PMCA is highly regulated by calmodulin (CaM), which activates this protein by binding to an auto-inhibitory region (5) and changes the conformation of the pump from an inhibited state to an activated one (5-7).

The current kinetic model for PMCA and SERCA proposes that enzymes exist in two main conformations: E_1 and E_2. After the binding of intracellular Ca^{2+} to high affinity sites, E_1 can be phosphorylated by ATP with formation of the intermediate E_1P. The conformational transition to E_2P leads to the release of Ca^{2+} to the opposite side of the membrane. The dephosphorylation of E_2P to E_2 and a new conformational transition to E_1 allow a new pump cycle (8, 9). Magnesium is necessary for optimal catalysis of PMCA (10) and SERCA (11). This ion accelerates the $E_2 \rightarrow E_1$ (11, 12) and the $E_1P \rightarrow E_2P$ transitions (13). Several ligands have been used for studying intermediates (EP) in these pumps. In PMCA, lanthanum (La^{III}) is known to prevent the Mg^{2+}- dependent transition $E_1P \rightarrow E_2P$, fixing the pump in E_1P (14, 15) while vanadate has been used for mimicking the E_2P state (16). Furthermore, beryllium fluoride (BeFx) (17), magnesium fluoride (MgFx) (18, 19) and aluminum fluoride (AlFx) (20) were useful in SERCA to elucidate the mechanism of ATP hydrolysis, because these phosphate analogues bind to the phosphorylation site mimicking the different steps of the E_2P dephosphorylation (21). In the presence of calcium and ADP, aluminum fluoride stabilizes the E_1P analogue conformation (22).

In this work, we study the effect of aluminum on PMCA purified from human erythrocytes -about 90% PMCA4 and 10% PMCA1 (23)- and SERCA isolated from skeletal muscle -mostly SERCA1 (24)-. Our results show that Al^{3+} can bind quickly and strongly to both pumps inhibiting the Ca^{2+}-ATPase activity. This binding is affected by Ca^{2+} in SERCA, but not in PMCA. In SERCA, Al^{3+} prevents the phosphorylation, while in PMCA it prevents the dephosphorylation of the pump. Our results suggest that, in the presence of calcium and ATP, Al^{3+} fixes PMCA in an E_2P analogue conformation. This is the first evidence of an inhibitor that stabilizes an E_2P analogue conformation with the phosphate covalently bound.

MATERIALS AND METHODS

Reagents - All chemicals used in this work were of analytical grade and purchased mostly from Sigma. Recently drawn human blood for the isolation of PMCA was obtained from the Hematology Section of Fundación Fundosol (Argentina). Blood donation in Argentina is voluntary, and therefore the donor provides informed consent for the donation of blood and for the subsequent legitimate use of the blood by the transfusion service.

Purification of PMCA from Human Erythrocytes - PMCA was isolated from calmodulin-depleted erythrocyte membranes by the calmodulin-affinity chromatography procedure (25). Protein concentration after purification was about 15µg/ml. No phospholipids were added at any step along the purification procedure. The purification procedure described preserves transport activity and maintains the kinetic properties and regulatory characteristics of the enzyme in its native condition (25).

SERCA Preparation-SERCA was directly solubilized with $C_{12}E_{10}$ (0.5%) from sarcoplasmic reticulum membranes prepared from rabbit skeletal muscle as described in Mangialavori et al. (24).

Measurement of Ca^{2+}-ATPase Activity - Ca^{2+}-ATPase activity was measured by following the release of inorganic phosphate from ATP as described previously by Fiske and Subbarrow (27) or by measuring the [^{32}P]Pi released from [γ^{32}P]ATP as described by Richards *et al*. (28). In each condition, the quantity of Pi released in the absence of calcium was subtracted from the Pi released in its presence. The reaction medium contained 120 mM KCl, 30 mM MOPS-K (pH 7.2 at 37°C), 120 µM $C_{12}E_{10}$, 35 µM DMPC and 30 µM EGTA. Optimal Ca^{2+}-ATPase activities of PMCA and SERCA in the mentioned medium were determined in the presence of 1.8 mM free Mg^{2+} and 80 µM free Ca^{2+} or 1 mM free Mg^{2+} and 10 µM free Ca^{2+}, respectively. When indicated, an aqueous five-fold concentration so-

lution of $AlCl_3$ was added to the reaction medium (named pre-incubation medium hereafter) containing PMCA or SERCA and was allowed to equilibrate for 5 min. The addition of $AlCl_3$ solutions does not change the pH of the pre-incubation medium. When necessary we dissolved $AlCl_3$ in an acidic pH and employed HEPES-acetate. The reaction was started by the addition of ATP-Mg^{2+} (final concentration of 2 mM for the non- radioactive assay and 30 μM for the radioactive one). The experimental set-up was adjusted to ensure that PMCA and SERCA (10 nM) initial velocity conditions were met. Measurements were carried out at 37ºC (non-radioactive assay) or 25ºC (radioactive assay).

For the time course experiments, the $AlCl_3$ the $AlCl_3$ solutions were added to the pre-incubation medium containing PMCA or SERCA and optimal concentrations of free Mg^{2+} and Ca^{2+} for each pump. After pre-incubation, Ca^{2+}-ATPase activity was started with 2 mM ATP-Mg. Due to the higher affinity of Al^{3+} for ATP, all the remaining aluminum binds to ATP, leaving free aluminum in the reaction medium (29).

Determination of Phosphorylated Intermediates - The phosphorylated intermediates (*E*P) were measured as the amount of acid-stable ^{32}P incorporated into the enzyme, according to the method described by Echarte et al. (30). The phosphorylation was measured at 25ºC in the same medium in which the Ca^{2+}-ATPase activities of PMCA and SERCA were determined. For PMCA, a condition in the presence of 100 μM $LaCl_3$ was included as control of the maximal amount of *E*P intermediate. The reaction was started by the addition of [γ-^{32}P]ATP under vigorous stirring, and after 30 seconds, it was stopped with an ice-cold solution of TCA (10% (w/v) final concentration). The tubes were centrifuged at 10,000 rpm for 5 min at 4ºC. The samples were then washed once with 7% TCA, 150 mM H_3PO_4 and once with double-distilled water and processed for SDS-PAGE. For this purpose, the pellets were dissolved in a medium containing 150 mM Tris-HCl (pH 6.5 at 14ºC), 5% SDS, 5% DTT, 10% glycerol, and bromophenol blue (sample buffer). Electrophoresis was performed at pH 6.5 (14ºC) in a 7.5% polyacrylamide gel. The reservoir buffer was 0.1 M sodium phosphate, pH 6.3, with 0.1% SDS. Gels were stained, dried and exposed to a Storage Phospho-Screen (*Amersham Biosciences*). Unsaturated autoradiograms were scanned with *Storm Molecular Image System* and stained gels were scanned with an *HP Scanjet G2410*. Analysis of the images was performed with *GelPro Analyzer*. *E*P quantification was achieved as described by Echarte et al. (30).

Dephosphorylation Procedure. Phosphorylation of PMCA was carried out at 4°C in the absence or in the presence of 25 μM $AlCl_3$. The reaction was started by the addition of 30 μM [γ-^{32}P]ATP under vigorous stirring. After 3 minutes, phosphorylation was stopped by the addition of 1 mM ADP or 0.5 mM ATP and enough DMPC, $C_{12}E_{10}$, ATP, and Mg^{2+} to maintain the phosphorylation conditions. Dephosphorylation was carried out at 4°C under stirring during the time periods described in the figures and stopped manually by adding 7% w/v TCA. After this, the samples were treated as was described in "*Determination of Phosphorylated Intermediates".*

Data analysis - Theoretical equations were fitted to the results by nonlinear regression based on the Gauss-Newton algorithm using commercial programs (Excel and Sigma-Plot for Windows, the latter providing not only the best fitting values of the parameters but also their standard errors). The goodness of fit of a given equation to the experimental results was evaluated by the corrected AIC criterion defined as $AIC_C = N \ln(SS/N) + 2P\,N/(N\text{-}P\text{-}1)$, where N is the number of data, P is the number of parameters plus one, and SS is the sum of weighted square residual errors. Unitary weights were considered in all cases and the best equation was chosen as that giving the lower value of AIC_C. The AIC criterion is based on Information Theory, and selects an equation among several possible equations on the basis of its capacity to explain the results using a minimal number of parameters.

RESULTS

Inhibition of Ca^{2+}-ATPase Activity of PMCA and SERCA by aluminum

PMCA and SERCA were first incubated with $AlCl_3$ in different concentrations and then 2 mM ATP-Mg was added. Details on the media composition are given under Experimental Procedures (Measurement of Ca^{2+}-ATPase Activity). The rate of Pi release was calculated from the slopes of the curves in the insets for both PMCA (Figure 1A) and SERCA (Figure 1B). A decreasing hyperbolic equation (Eq. 1) was fitted to the experimental results (continuous lines),

$$v = \frac{V_0 K_{AlCl_3}}{K_{AlCl_3} + [AlCl_3]} \qquad \text{Eq. 1}$$

where V_0 is the Ca^{2+}-ATPase activity in the absence of $AlCl_3$ and K_{AlCl_3} is the concentration of $AlCl_3$ needed for half-maximal effect. The values obtained for K_{AlCl_3}in PMCA and SERCA were 8.3 ± 0.5 µM and 10.1 ± 0.7 µM, respectively. These results show that $AlCl_3$ inhibits both pumps with similar apparent affinities.

Effects of calcium and magnesium on the inhibition of PMCA and SERCA by aluminum

We investigated the interactions of Al^{3+} with Mg^{2+} and Ca^{2+} binding sites in both PMCA and SERCA. PMCA was pre-incubated in the presence of different concentrations of Ca^{2+} and $AlCl_3$, at 1.85 mM Mg^{2+}, or different concentrations of Mg^{2+} and $AlCl_3$, at 70 µM Ca^{2+}. After 5 minutes, Ca^{2+}-ATPase reaction was started by adding 2 mM ATP-Mg. Figure 2A shows the Ca^{2+}-ATPase activity of PMCA under these experimental conditions. In all cases, experimental data were described by the rectangular hyperbola (Eq. 2),

$$v = \frac{V_{\max} x}{K_{0.5} + x} \qquad \text{Eq. 2}$$

where V_{max} is the Ca^{2+}-ATPase activity when the Ca^{2+} concentration, x, tends to infinity and $K_{0.5}$ represents the [Ca^{2+}] at which the half-maximum effect is achieved. The best fitting values of $K_{0.5}$ and V_{max} are plotted as a function of $AlCl_3$ concentration in Figures 2E and I.

The same experimental approach was used with SERCA –at 1 mM free Mg^{2+}-. Ca^{2+}-ATPase activity is shown in Figure 2B. Values of $K_{0.5}$ and V_{max}, obtained are plotted in Figures 2F and J, respectively. In agreement with our previous reports (31), the $K_{0.5}$ for calcium of PMCA and SERCA reconstituted in $C_{12}E_{10}$/DMPC mixed micelles were 12.1 ± 0.5 µM and 0.92 ± 0.05 µM, respectively. In PMCA, when the concentration of $AlCl_3$ increases, $K_{0.5}$ for Ca^{2+} is not significantly modified (Figure 2E) and V_{max} decreases (Figure 2I), suggesting that Ca^{2+} does not protect against the binding of aluminum to PMCA. In SERCA, $AlCl_3$ produces an increase of $K_{0.5}$ for Ca^{2+} (Figure 2F), while V_{max} remains approximately constant (Figure 2J). This result shows that Ca^{2+} protects SERCA from aluminum binding, suggesting that Al^{3+} binds to the Ca^{2+} transport site(s) of SERCA.

Using a similar approach, we evaluated the effect of magnesium on the binding of aluminum to the pumps (Figures 2C and D). The $K_{0.5}$ for free magnesium, Mg^{2+}, for PMCA (G) and SERCA (H) are not significantly modified by the presence of $AlCl_3$ whereas V_{max} decreased (Figures 2K and L, respectively). These results show that Al^{3+} is not a competitive inhibitor of Mg^{2+} neither in PMCA nor in SERCA.

On the reversibility of aluminum inhibition

The fact that inhibition by $AlCl_3$ in PMCA is not accompanied by changes of $K_{0.5}$ for Mg^{2+} and Ca^{2+} suggests that aluminum might be either a non-competitive inhibitor or an irreversible inhibitor of the pump. In order to investigate the reversibility of the inhibition, PMCA was pre-incubated with a concentration of $AlCl_3$ in the $K_{0.5}$ of inhibition and then diluted fifteen times. After different times, activity was determined by adding 2 mM ATP-Mg (Figure 3A). The pump activity remained constant indicating that enzyme-aluminum complex (*E*Al) does not dissociate in the times assayed. This behavior was also observed at different aluminum concentrations where PMCA activity was the same whether the pump was diluted or not after inhibition (Figure 3A *inset*). This result indicates that aluminum behaves like an irreversible inhibitor of PMCA.

In agreement with the result described in Figures 2F and J, SERCA Ca^{2+}-ATPase activity recovers, indicating that the *E*Al complex dissociates (Figure 3B). An exponential function was fitted to the experimental data,

$$v = v_0 + a(1 - e^{-kt}) \qquad \text{Eq. 3}$$

where V_0 is the Ca^{2+}-ATPase activity when the time after dilution tends to zero, *a* is the maximal change in Ca^{2+}-ATPase activity and *k* is the rate coefficient of the Ca^{2+}-ATPase activity recovery. The values of the parameters V_0, *a* and *k* were 57.2 ± 11%; 42.8 ± 16.8% and 0.02 ± 0.008 min^{-1}, respectively. The calculated half-time for the dissociation of the *E*Al complex is about 27 minutes, indicating that aluminum is a slowly-reversible inhibitor of SERCA.

Time course for inhibition of PMCA and SERCA by aluminum

To investigate the mechanisms of inhibition of the pumps by aluminum, PMCA (Figure 4A) and SERCA (Figure 4B) were pre-incubated at different times with increasing concentrations of $AlCl_3$. Then, the Ca^{2+}-ATPase reaction was started by adding ATP-Mg (2 mM). Note that, due to its combination with ATP (29), free aluminum concentration rapidly drops in the reaction medium; consequently, this strategy is similar to diluting the samples. At low concentrations, the complex formed, ATP-Al, affects neither PMCA nor SERCA Ca^{2+}-ATPase activities (Figure 4C).

Experimental data were described by the sum of two decreasing exponential functions of time:

$$v = a.e^{-k_1 t} + b.e^{-k_2 t} \qquad \text{Eq. 4}$$

where *a* and *b* are the maximal changes of the fast and slow phases of Ca^{2+}-ATPase activity, and k_1 and k_2 are the rate coefficients of each phase, respectively.

Aluminum in aqueous solution is solvated with water molecules. This form is known as free aluminum ($Al(H_2O)_6^{3+}$ (or simply, Al^{3+}) and is favored at acidic pH. When the pH rises, aluminum is complexed with OH^- from deprotonation of water molecules ($Al(OH)_n$). Moreover, aluminum precipitates as hydroxides and forms dissolved complexes with different polymerization grade (Al_n) (32). Then, hydrolysis of aluminum in aqueous solutions is extremely complex and depends, among others, on aluminum concentration, pH, temperature and time (33, 34).

The fluorescence change of Lumogallion after addition of $AlCl_3$ (Figure S1) suggests that only a fraction of $AlCl_3$ in the solutions binds rapidly to the probe, while the rest seems to form aqueous complexes that slowly release the species that can bind to the probe. Assuming that Al^{3+} is the inhibitory species, this result gives support to the biphasic time courses for the inhibition of the Ca^{2+}-ATPase activity.

The concentration of species that inhibit SERCA and PMCA increases at acidic pH

In order to confirm whether the inhibition of the pumps depends on the relative amount of different aluminum species, the same concentration of $AlCl_3$ was dissolved in media of different pH. In this way, each solution has the same amount of $AlCl_3$ but the concentrations of the different species vary, e.g. the concentration of Al^{3+} increases at lower pH. These different solutions were incorporated into the pre-incubation medium at pH 7.3. A solution without $AlCl_3$ was used to control that the addition of media with different pH does not modify the final pH (and therefore the Ca^{2+}-ATPase activity, Figures 5A and B). The percentage of inhibition of the pumps depends on the pH where the $AlCl_3$ solution was dissolved and then added to the pre-incubation medium. These results agree with the increase in the amplitude of the fast phase of the time course of inhibition at lower pH values (Figure S2, panel C). Further, the results also demonstrate that the aluminum-enzyme complex is very stable since it does not dissociate upon changing the pH.

In another experiment, we measured the Ca^{2+}-ATPase activity at different pH values in the absence of $AlCl_3$ or in the presence of 10 or 25 µM $AlCl_3$ (Figures 5C and D). As expected, Ca^{2+}-ATPase activity was maximal at neutral pH both for PMCA and SERCA (35, 36). Figures 5E and F show that the percentage of inhibition of the pumps by $AlCl_3$ increases at lower pH, in agreement with the results in panels A and B.

These results can be explained if we consider that: (1) Al^{3+} (and probably also $Al(OH)^{2+}$ and $Al(OH)_2^+$, hereafter referred to as Al^{3+}, for simplicity) is the main inhibitory species of both pumps; (2) in the biphasic time courses observed in Figure 4, the fast phase is related to the amount of soluble Al^{3+} present in the medium while the slow phase is related to the release of Al^{3+} from other species (Figure S1); and (3) once formed the *E*Al complex does not dissociate significantly during the time of

the experiments. According to this interpretation, the inhibition of the pumps by aluminum can be described by the following mechanism:

$$Al^{3+} + E \underset{k_{-1}}{\overset{k_1}{\rightleftharpoons}} EAl^{3+}$$

where the value of k_{-1} is close to zero in PMCA, while in SERCA is such that it can be measured from the results in Figure 3B. This means that, for the time length used in our experiments, inhibition by Al^{3+} of PMCA and SERCA can respectively be considered as irreversible and slowly reversible processes.

Aluminum stabilizes phosphorylated intermediates (*E*P) in PMCA but not in SERCA

PMCA and SERCA form acid-stable phosphorylated intermediates, E_1P and E_2P that interconvert during the reaction cycle. Measurement of *E*P, i.e. the aggregated amount of E_1P and E_2P, is of great relevance for the characterization of partial reactions of the enzyme cycle and has provided valuable information for the elucidation of the mechanism of its modulators. To further characterize the inhibition by aluminum, we studied the dependence of the levels of phosphorylated intermediates of PMCA and SERCA on $AlCl_3$ concentration.

Figure 6A shows that the amount of PMCA phosphorylated intermediates increases with the concentration of $AlCl_3$ along the following hyperbolic function

$$EP = EP_0 + \frac{(EP_{max} - EP_0).[AlCl_3]}{K_{AlCl_3} + [AlCl_3]} \quad \text{Eq. 5}$$

where, EP_0 and EP_{max} are the amounts of PMCA phosphorylated in the absence of $AlCl_3$ and in the presence of non-limiting concentrations of the inhibitor, respectively, and K_{AlCl_3} is the concentration of $AlCl_3$ at which $EP = (EP_{max} + EP_0)/2$. The value of EP_0 was taken as 100%. The best fitting values for EP_0, EP_{max} and K_{AlCl_3} were 100.7 ± 4.8%; 199.9 ± 7.4% and 9.4 ± 1.6 µM, respectively. In PMCA, lanthanum (La^{III}) is known to prevent the Mg^{2+}- dependent transition $E_1P \rightarrow E_2P$, producing the maximal level of *E*P (14, 15). Therefore, we included a control where $AlCl_3$ was replaced by a non-limiting concentration of $LaCl_3$. We found a level of *EP* of 172.8 ± 6.7%. In parallel experiments, we measured Ca^{2+}-ATPase activity (Figure 6C). As expected, the K_{AlCl_3} value obtained from Ca^{2+}-ATPase activity at 30 µM ATP-Mg (7.7 ± 2.3 µM) was not significantly different from that obtained from the *E*P measurement. Hereafter, we will refer to the phosphorylated intermediate of PMCA stabilized in the presence of $AlCl_3$ as *E*PAl.

Conversely, *E*P in SERCA decreases with increasing concentrations of $AlCl_3$ (Figure 6B). A decreasing hyperbolic function (Eq. 6) was fitted to the experimental data

$$EP = \frac{EP_0.K_{AlCl_3}}{K_{AlCl_3} + [AlCl_3]} \quad \text{Eq. 6}$$

In that equation, EP_0 is the amount of SERCA phosphorylated intermediate in the absence of aluminum and K_{AlCl3} is the concentration of $AlCl_3$ for half-maximum effect. The best fitting values for EP_0 and K_{AlCl3} were 102.3 ± 1.2% and 4.5 ± 0.3 µM, respectively. The value of K_{AlCl3} obtained from the measurement of Ca^{2+}-ATPase activity at 30 µM ATP-Mg was 5.6 ± 0.9 µM (Figure 6D).

Figures 6E and F show the residence time of *E*P (t(*E*P)) calculated as the ratio between the *E*P levels and Ca^{2+}-ATPase activity. Under the experimental conditions tested, the residence time depends exclusively on the rate of dephosphorylation of E_2P and the rate of interconversion between E_1P and E_2P (10). For PMCA, an increase of $AlCl_3$ concentration produces an increase of the residence time of *E*P (t(*E*P)), which indicates a decrease in the rate of breakdown of *E*P rather than an increase in the phosphorylation rate. In SERCA, t(*E*P) remains constant with the $AlCl_3$ concentration suggesting that the phosphorylated intermediates are not involved in the inhibition by aluminum. This result

is in agreement with the protective effect of calcium shown above (Figures 2, panels B, F and J) suggesting that aluminum inhibition in SERCA is due to the competition for Ca^{2+} binding site(s).

Effect of ADP and ATP on the *E*PAl dephosphorylation

Figure 7A shows the time course of *E*P decay after adding 1 mM ADP. Decay presented a biphasic behaviour both in the absence (control) and in the presence of $AlCl_3$ (*E*PAl complex). We fitted the sum of two exponential equations to the experimental data:

$$EP = EP_f . e^{-k_1 t} + EP_s . e^{-k_2 t} \quad \text{Eq. 7}$$

where EP_f and EP_s are the amplitudes and k_1 and k_2 are the apparent rate constants of the fast and slow *E*P decay components, respectively. Results are expressed as a percentage of the amount of *E*P in the absence of $AlCl_3$ at time zero. The best fitting values of the parameters are detailed in Table 1.
It is generally accepted that, in the dephosphorylation by ADP, the fast component is due to dephosphorylation of E_1P while the slow component reflects the $E_2P \rightarrow E_1P$ transition. The amplitude of fast (EP_f) and the slow (EP_s) components are an estimation of the steady-state amount of E_1P and E_2P, respectively. The value of EP_f decreases from 66% to 40% in the presence of $AlCl_3$ suggesting that the $E_1P \leftrightarrow E_2P$ equilibrium is displaced toward E_2P. Figure 2C shows that *E*PAl also decayed in a biphasic way after adding 0.5 mM ATP. Eq. 7 was fitted to the experimental data, but in this case, the fast component is due to dephosphorylation of E_2P while the slow component reflects the $E_1P \rightarrow E_2P$ transition phase (37). The best fitting values of the parameters are shown in Table 1. According to the results shown in panel A, about 65% of *E*PAl has a conformation analogue to E_2P.

DISCUSSION

Although with a different stoichiometry and regulation (35, 36, 38), PMCA and SERCA are P-ATPases that transport Ca^{2+} against the electrochemical gradient using the energy of ATP hydrolysis. They form phosphorylated intermediates during their reaction cycles. Phosphorylation, transition between phosphoenzyme conformers and dephosphorylation steps depend on the binding of Mg^{2+}. Our results show that Al^{3+} stabilizes a phosphorylated intermediate of PMCA whereas it binds to a dephosphorylated intermediate in SERCA. Both PMCA (39) and SERCA (40) bind ATP with high affinity in the absence of Ca^{2+}. However, Ca^{2+} binding is required for the enzyme activation, even if Mg^{2+} is present. This is because Ca^{2+} is required for ATP γ-phosphate to reach the *Asp* residue, which allows the phosphorylation of the enzyme (40). Therefore, the fact that in PMCA the *E*Al complex becomes phosphorylated suggests that the pump acquires the correct conformation. Following a similar line of argument, the conformation of the *E*Al complex in SERCA is clearly not suitable for phosphorylation. This conclusion and the protective effect produced by Ca^{2+} suggest that Al^{3+} could bind in SERCA to the Ca^{2+} binding site.

In PMCA, Mg^{2+} favors the conversion $E_1P \rightarrow E_2P$ (13) and, as in SERCA (11), it accelerates the phosphorylation displacing the E_1-E_2 equilibrium towards E_1. In SERCA, Sørensen et al. (41), proposed that ATP reacts by an associative mechanism mediated by two Mg^{2+} ions to form an aspartyl-phosphorylated intermediate state (E1~P). Cornelius et al. (42) suggested that Al^{3+} can replace Mg^{2+} in its specific site in Na^+/K^+-ATPase. Our results show that Al^{3+} inhibits PMCA activity by stabilizing a phosphorylated intermediate, suggesting that it could replace Mg^{2+} and prevent the dephosphorylation of the enzyme. The possibility that Al^{3+} could inhibit through the binding to ATP can be ruled out by the experiments in this paper (see Figure 6). In PMCA, La^{III} replaces Mg^{2+} preventing the $E_1P \rightarrow E_2P$ isomerization step thus increasing both the PMCA *E*P level (14, 15) and the Ca^{2+} occlusion (43). According to the fact that La^{III} stabilizes the E_1P conformation, *E*PLa is quickly dephosphorylated in the presence of ADP with a monoexponential behaviour (15), The time courses of *E*PAl dephosphorylation in the presence of ADP or ATP show a biphasic behaviour indicating that this complex is composed by both E_2P and E_1P. However, unlike for La^{III}, 65% of *E*PAl is in the E_2P conformation.

CONCLUSION

In short, we show that aluminum inhibits SERCA by a slowly reversible mechanism in which Al^{3+} displaces Ca^{2+} from its binding site. Conversely, in PMCA Al^{3+} inhibits the dephosphorylation step fixing the pump in a very stable complex composed mainly by the conformer E_2P.

Acknowledgements: We thank the help of Professor Dr. Delia Takara in SERCA purification and the support provided by Hematology Section of Fundación Fundosol (Argentina).

Competing interests: The authors declare no competing or financial interests.

REFERENCES

1. Kawahara, M., and Kato-Negishi, M. (2011) Link between Aluminum and the Pathogenesis of Alzheimer's disease: The Integration of the Aluminum and Amyloid Cascade Hypotheses. *Int. J. Alz-heimers Dis.*, **2011**, Article ID 276393, 17 pages doi:10.4061/2011/276393
2. Martin, B. R. (1986) The Chemistry of Aluminum as Related to Biology and Medicine. *Clin. Chem.* **32/10**, 1797-1806
3. Strehler, E. E., Caride, A. J., Filoteo, A. G., Xiong, Y., Penniston, J. T., and Enyedi, A. (2007) Plasma Membrane Ca^{2+}- ATPases as Dynamic Regulators of Cellular Calcium Handling. *Ann. N. Y. Acad. Sci*. **1099**, 226-236
4. Toyoshima, C. (2009) How Ca^{2+}-ATPase pumps ions across the sarcoplasmic reticulum membrane. *Biochim. Biophys. Acta* **1793**, 941-946. 10
5. Sarkadi B., Enyedi, A., Foldes-Papp, Z., and Gárdos, G. (1986) Molecular characterization of the in situ red cell membrane calcium pump by limited proteolysis. *J. Biol. Chem.* **261**, 9552-9557
6. Corradi, G.R., and Adamo, H.P. (2007) Intramolecular fluorescence resonance energy transfer between fused autofluorescent proteins reveals rearrangements of the N- and C-terminal segments of the plasma membrane Ca^{2+} pump involved in the activation. *J. Biol. Chem.* **282**, 35440-35448
7. Mangialavori, I.C., Villamil-Giraldo A.M., Pignataro, M.F., Ferreira-Gomes M.S., Caride A.J., and Rossi J.P.F.C. (2011) Plasma membrane calcium pump (PMCA) differential exposure of hydrophobic domains after calmodulin and phosphatidic acid activation. *J. Biol. Chem.* **286**, 18397-18404
8. Rega, A.F., and Garrahan, P.J. (1986) The Ca^{2+} Pump of Plasma Membranes, CRC Press Inc., Boca Raton, FL
9. de Meis L, and Vianna, A.L. (1979) Energy interconversion by the Ca2+-dependent ATPase of the sarcoplasmic reticulum. *Annu Rev Biochem.* **48**, 275-92.
10. Echarte, M. M., Rossi, R. C. and Rossi, J.P. (2007) Phosphorylation of the plasma membrane calcium pump at high ATP concentration. On the mechanism of ATP hydrolysis. *Biochemistry.* **46**, 1034-1041
11. Picard, M., Jense, A. M., Sørensen, T. L., Møller, J. V., and Nissen, P. (2007) Ca2+ versus Mg2+ coordination at nucleotide-binding site of the sarcoplasmic reticulum Ca^{2+}-ATPase. *J. Mol. Biol.* **368**, 1-7
12. Champeil, P., Gingold, M. P., Guillain, F., and Inesi, G. (1983) Effect of magnesium on the calcium-dependent transient kinetics of sarcoplasmic reticulum ATPase, studied by stooped flow fluorescence and phosphorylation. *J. Biol. Chem.* **258**, 4453-4458
13. Adamo, H. P., Rega, A. F., and Garrahan, P. J. (1990) Magnesium-ions accelerate the formation of the phosphoenzyme of the (Ca^{2+}-Mg^{2+})-activated ATPase from plasma membranes by acting on the phosphorylation reaction. *Biochem Biophys Res Commun.* **169**, 700-705
14. Luterbacher, S., and Schatzmann, H. J. (1983) The site of action of La^{3+} in the reaction cycle of human red cell membrane Ca^{2+}-pump ATPase. *Experientia*. **39**, 311-312

15. Herscher, C. J., and Rega, A. F. (1996) Pre-steady-state kinetic study of the mechanism of inhibition of the plasma membrane Ca($^{2+}$)-ATPase by lanthanum. *Biochemistry.* **35**, 14917-14922
16. Rossi, J.P.F.C., Garrahan, P.J., and Rega, A.F. (1981) Vanadate inhibition of active Ca^{2+} transport across human red cell membranes. *Biochim. Biophys. Acta.* **648**, 145-150
17. Murphy, A. J., and Coll, R. J. (1993) Formation of a stable inactive complex of the sarcoplasmic reticulum calcium ATPase with magnesium, beryllium, and fluoride. *J. Biol. Chem.* **268**, 23307-23310
18. Murphy, A. J., and Coll, R. J. (1992) Fluoride binding to the calcium ATPase of sarcoplasmic reticulum converts its transport sites to a low affinity, lumen-facing form *J. Biol. Chem.***267**, 16990-16994
19. Yamasaki, K., Daiho, T., and Suzuki, H. (2002) Remarkable stability of solubilized and delipidated sarcoplasmic reticulum Ca^{2+}-ATPase with tightly bound fluoride and magnesium against detergent-induced denaturation. *J. Biol. Chem*. **277**, 13615-13619
20. Troullier, A., Girardet, J.-L., and Dupont, Y. (1992) Fluoroaluminate complexes are bifunctional analogues of phosphate in sarcoplasmic reticulum Ca^{2+}-ATPase. *J. Biol. Chem.* **267**, 22821-22829
21. Danko, S., Yamasaki, K., Daiho, T., and Suzuki, H. (2004) Distinct Natures of Beryllium Fluoride-bound, Aluminum Fluoride-bound, and Magnesium Fluoride-bound Stable Analogues of an ADP-insensitive Phosphoenzyme Intermediate of Sarcoplasmic Reticulum Ca^{2+}-ATPase: Changes in cat-alytic and transport sites during phosphoenzyme hydrolysis. *J. Biol. Chem*. **279**, 14991-14998
22. Toyoshima, C., Nomura, H., and Tsuda, T. (2004) Crystal structure of the SR Calcium Pump with bound aluminium fluoride, ADP and calcium. *Nature*. 432, 361-368
23.Strehler, E.E., James, P., Fisher, R., Vorherr, T., Filoteo, A. G., Penniston, J. T., and Carafoli, E. J. (1990) Peptide sequence analysis and molecular cloning reveal two pump isoforms in the human erythrocyte membrane. *J. Biol. Chem.* **265**, 2835-2842
24. Lytton, J., Westlin, M., Burk, S.E., Shull, G. E., and MacLennan, D. H. (1992) Functional comparisons between isoforms of the sarcoplasmic or endoplasmic reticulum family of calcium pumps. *J. Biol. Chem*. **267**, 14483–14489
25. Niggli, V., Penniston, J. T., and Carafoli, E. (1979) Purification of the (Ca^{2+}-Mg^{2+})-ATPase from human erythrocyte membranes using a calmodulin affinity column. *J. Biol. Chem.* **254**, 9955-9958
26. Mangialavori, I.C., Villamil-Giraldo, A.M., Marino-Buslje, C.M., Ferreira-Gomes, M.F., Caride, A.J., Rossi, J.P.F.C. (2009) A new conformation in sarcoplasmic reticulum calcium pump and plasma membrane Ca2+ pumps revealed by a photoactivatable phospholipidic probe. *J Biol Chem*. **284**, 4823-4828
27. Fiske, C. H.,and SubbaRow, Y. (1925) The colorimetric determination of phosphorous. *J Biol Chem*. **179**, 66-67
28. Richards, D. E., Rega, A. F., and Garrahan, P. J. (1978) Two classes of site for ATP in the Ca2+-ATPase from human red cell membranes. *Biochim. Biophys. Acta* **511**, 194-201
29. Nelson D. J. (1996) Aluminum complexation with nucleoside di- and triphosphates and implication in nucleoside binding proteins. *Coord Chem Rev*. **149**, 95-111
30. Echarte, M. a. M., Levi, V., Villamil, A. M. a., Rossi, R. C., and Rossi, J. P. F. C. (2001) Quantitation of Plasma Membrane Calcium Pump Phosphorylated Intermediates by Electrophoresis. *Anal Biochem*. **289**, 267-273A
31. Mangialavori, I.C., Ferreira-Gomes, M.F., Pignataro, M.F., Strehler, E.E., and Rossi, J.P.F.C. (2010) Determination of the dissociation constants for Ca^{2+} and calmodulin from the plasma membrane Ca^{2+} pump by a lipid probe that senses membrane domain changes. *J. Biol. Chem*. **285**, 123-130
32. Feng C, Bi Z, Tang H. (2015) Electrospray ionization time-of-flight mass spectrum analysis method of polyaluminum chloride flocculants. *Environ. Sci. Technol*. **49**, 474-80
33. Bi S., Wang,C., Cao, Q., and Zhang, C. (2004) Studies on the mechanism of hydrolysis and polymerization of aluminum salts in aqueous solution: correlations between the "Core-links" model and "Cage-like" Keggin-Al_{13} model. *Coord. Chem. Rev.* **248**, 441-455

34. Maki, H., Sakata, G., and Mizuhata, M. (2017) Quantitative NMR of quadrupolar nucleus as a novel analytical method: hydrolysis behaviour analysis of aluminum ion. *Analyst*. DOI: 10.1039/c7an00067g
35. Yu X, Carrol S, Rigoult J and Inesi G (1993) H^+ countertransport and Electrogenicity of the sarcoplasmic reticulum Ca^{2+} pump in reconstituted proteoliposomes. *Biophys. J.* **64**, 1232-1242
36. Tadini-Buoninsegni, F., Bartolommei, G., Moncelli, M. R., Guidelli, R., and Inesi, G. (2006) Presteady State Electrogenic Events of Ca^{2+}-H^+ Exchange and Transport by the Ca^{2+}-ATPase. *J. Biol. Chem.* **281**, 37720-37727
37. Herscher, C. J., Rega, A. F., and Garrahan, P. J. (1994) The dephosphorylation reaction of the Ca^{2+}-ATPase from plasma membranes. *J. Biol. Chem.* **269**, 10400-10406
38. Rossi, J. P., and Schatzmann, H. J. (1982) Is the res cell calcium pump electrogenic? *J Phisiol.* **327**, 1-15
39. Mangialavori, I. C., Ferreira-Gomes, M. S, Saffioti, N. A., Gonzalez-Lebrero, R. M., Rossi, R. C., and Rossi, J. P. (2013) Conformational changes produced by ATP binding to the plasma membrane calcium pump. *J. Biol. Chem.* **288**, 31030-31041
40. Inesi, G., Levis, D., Ma, H., and Prasad, A. (2006) Concerted conformational effects of Ca^{2+} and ATP are required for activation of sequential reactions in the Ca^{2+}-ATPase (SERCA) catalytic cy-cle. *Biochemistry* **45**, 13769-13778
41. Sørensen, T. L., Møller, J. V., and Nissen, P. (2004) Phosphril transfer and calcium occlusion in the calcium pump. *Science* **304**, 1672-1675
42. Cornelius, F., Mahmmoud, Y. A., and Toyoshima, C. (2011) Metal Fluoride Complexes of Na,K-ATPase: Characterization of fluoride-stabilized phosphoenzyme analogues and their Interaction with cardiotonic steroids. *J. Biol. Chem.* **286,** 29882-29892
43. Ferreira-Gomes, M. S., Gonzalez-Lebrero, R., de la Fuente, M. C., Strehler, E. E., Rossi, R. C., and Rossi, J. P. (2011) Calcium occlusion in plasma membrane Ca^{2+} ATPase *J. Biol. Chem.* **286**, 32018-32025

FOOTNOTES

This work was supported by Agencia Nacional de Promoción Científica y Tecnológica (PRESTAMO BID-PICT-2015-0067), Consejo Nacional de Investigaciones Científicas y Técnicas (PIP 0250) and Universidad de Buenos Aires, Ciencia y Técnica. (Argentina).

Table 1. Effect of ADP and ATP on the *E*P dephosphorylation

	EP_f (%)	k_1 (s^{-1})	EP_s (%)	k_2 (s^{-1})
*E*P *plus* ADP	65,8 ± 9,1	2,0 ± 0,8	34,2 ± 6,9	0,041 ± 0,030
*E*PAl *plus* ADP	80,4 ± 7,8 (39)	1,4± 0,4	116,2 ± 6,2 (61)	0,025 ± 0,012
*E*PAl *plus* ATP	125,8 ± 5,2 (64)	0,44 ± 0,06	73,8 ± 3,1 (36)	0,002 ± 0,001

Best values of the parameters after fitting Eq. 7 to the experimental data shown in Figures 7A and 7C. The value of *E*P obtained in the absence of $AlCl_3$ at zero time of dephosphorylation was fixed as 100%. The percentages of E_2P or E_1P relative to the total amount of *E*PAl are shown in brackets.

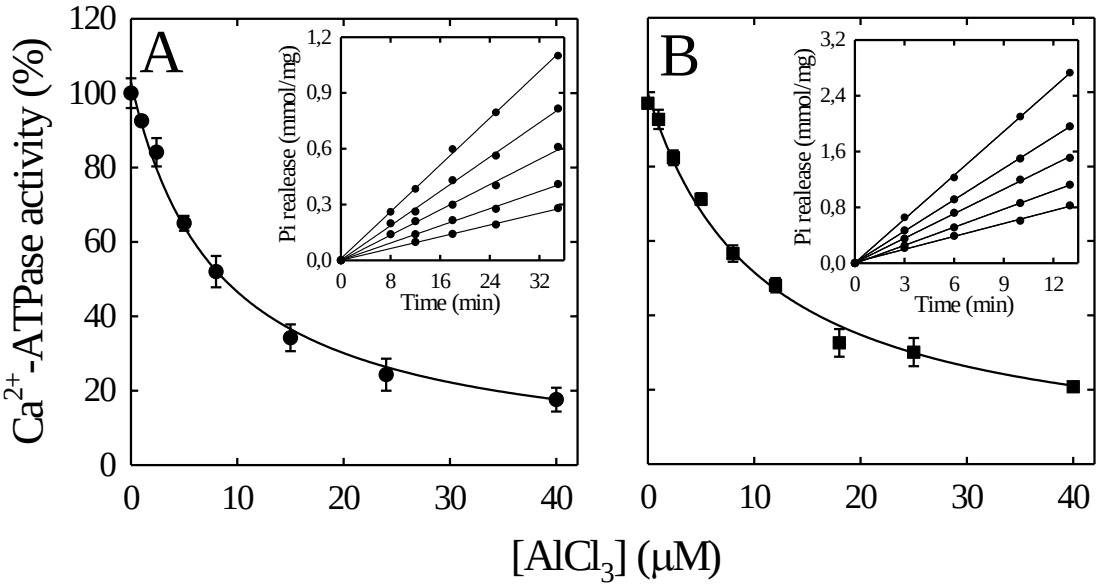

Figure 1: Ca^{2+}-ATPase activity of PMCA (**A**) and SERCA (**B**) as a function of $AlCl_3$ concentration**.** Free Mg^{2+} and free Ca^{2+} concentrations were respectively 1.8 mM and 70 µM (panel A) or 1 mM and 10 µM (panel B). Ca^{2+}-ATPase activity was determined from the slope of the curve of Pi release as function of time. *Inset* shows a representative experiment where (*from top to bottom*) 0; 3; 6; 12 and 25 µM $AlCl_3$ were assayed. Ca^{2+}-ATPase activity in the absence of $AlCl_3$ was defined as 100%. In both panels, continuous line is the graph of Eq. 1 for the best-fitting values of the parameters. Results are representative of eight independent experiments performed in duplicate.

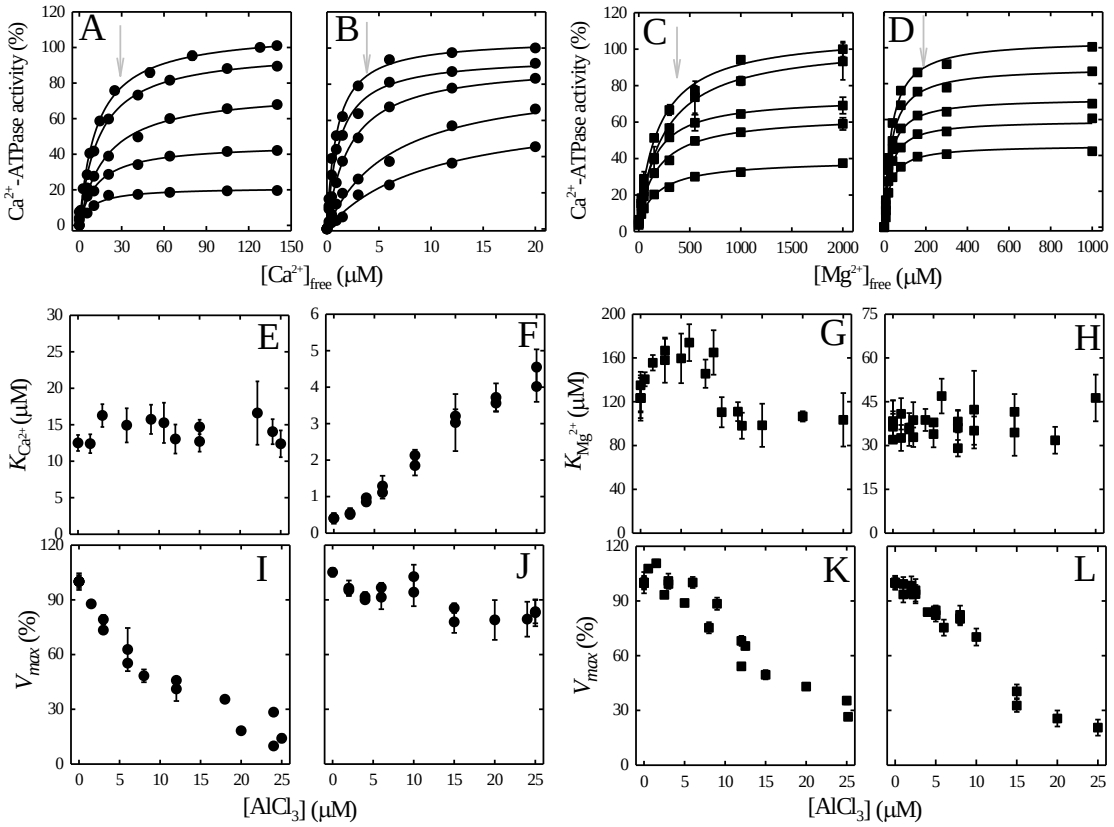

Figure 2: Effect of $AlCl_3$ on apparent affinity of PMCA and SERCA for Ca^{2+} and Mg^{2+}. Increasing $AlCl_3$ concentrations (*from top to bottom*: 0; 3; 8; 15; 25 μM (A) or 0; 2.5; 5; 10; 20 μM (B)) were added to the pre-incubation medium containing PMCA **(A)** or SERCA **(B)** in the presence of different free Ca^{2+} concentrations. Free Mg^{2+} concentration was 1.85 mM in (A) and 1 mM in (B). After 5 min., Ca^{2+}-ATPase activity was determined as described before. Maximal velocity (V_{max}) and apparent affinity for Ca^{2+} (K_{Ca}^{2+}) of PMCA and SERCA were obtained from the fitting of the Eq.2 to the experimental data of A and B and plotted as a function of $AlCl_3$ concentration in **E** and **F** or **I** and **J**, respectively. (**C** and **D**). Increasing $AlCl_3$ concentrations (*from top to bottom*: 0; 2; 5; 10; 18 μM (C) or 0; 2; 4; 8; 12; 15 μM (D)) were added to the pre-incubation medium containing PMCA **(C)** or SERCA **(D)** in the presence of different free Mg^{2+} concentrations. Free Ca^{2+} concentration was 70 μM in (C) and 10 μM in (D). Following the experimental approach described above: **G** and **H** show the values of K_{Mg}^{2+} and, **K** and **L** show the values of V_{max} obtained for PMCA and SERCA, respectively. Panels A to D are representative experiments. Panels E to L corresponds to the values obtained from four to six independent experiments.

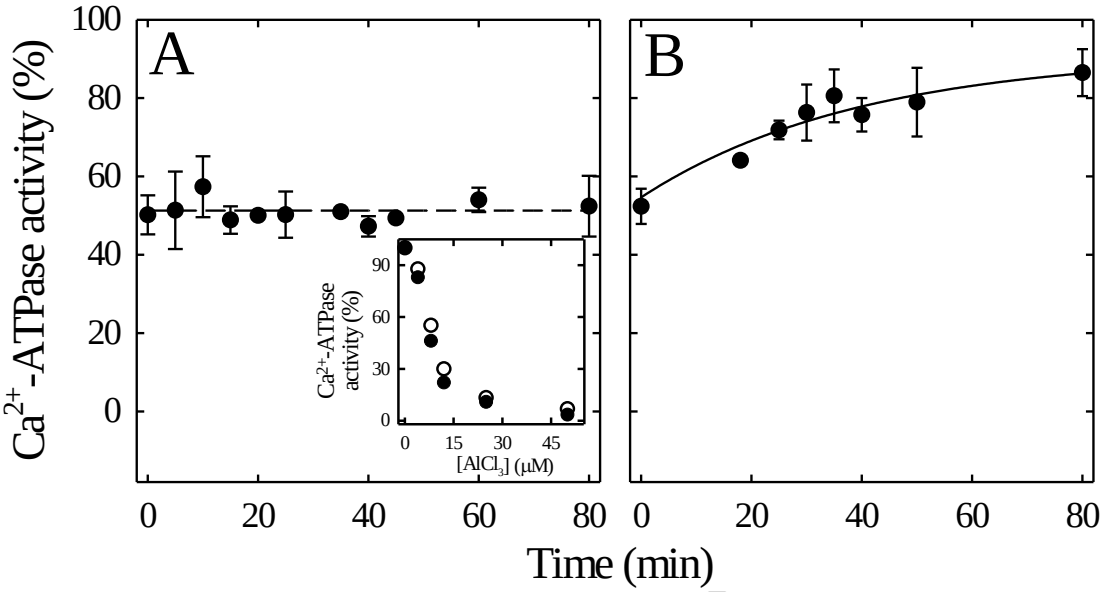

Figure 3: Reversion of $AlCl_3$ inhibition: PMCA (**A**) and SERCA (**B**) were pre-incubated with 10 μM $AlCl_3$. At "time zero" the pre-incubation medium was diluted 15 times, after different times, aliquots were taken, and Ca^{2+}-ATPase activity was determined. For PMCA, Ca^{2+}-ATPase activity was constant (dotted line). For SERCA, Ca^{2+}-ATPase activity values were well described by the equation Eq. 4 (continuous line). ***Inset in A***: Representative experiment in which the pre-incubation medium containing PMCA and different $AlCl_3$ concentration was diluted 15 times (open circles) or not (closed circles) with the solution containing ATP. Results show in A and B correspond to the average ± SD of two independent experiments.

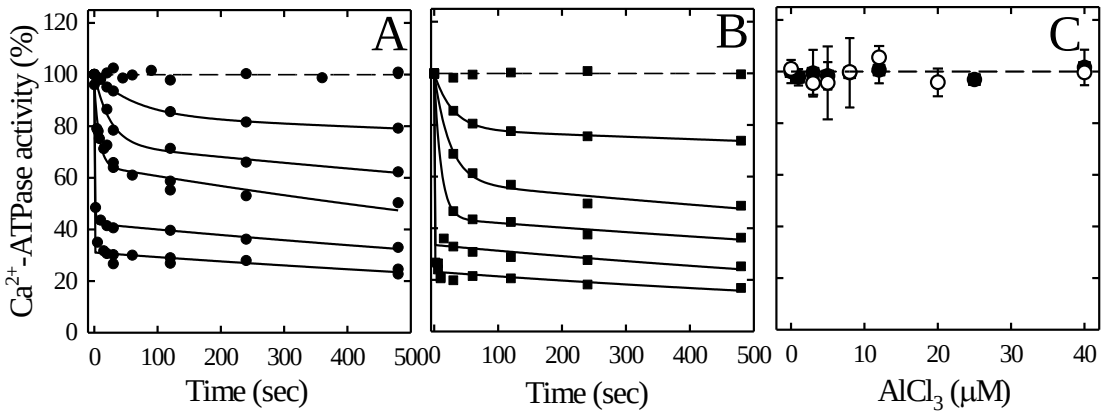

Figure 4: Time course of $AlCl_3$ inhibition of PMCA (**A**) and SERCA (**B**). The pumps were pre-incubated with different $AlCl_3$ concentrations (*PMCA*: 0; 3; 6; 10; 15 and 25 μM and, SERCA 0; 5; 10; 15; 25 and 40 μM), then, Ca^{2+}-ATPase activity reaction was initiated by adding 2 mM ATP-Mg. The continuous lines represent the fitting of Eq. 2 to experimental data. (**C**) Ca^{2+}-ATPase activity of PMCA (open circles) and SERCA (closed square) when different $AlCl_3$ concentrations were added after starting the reaction with 2 mM ATP-Mg. Figures. A and B are representative of three independent experiments and Figure C corresponds to average ± SD of two independent experiments.

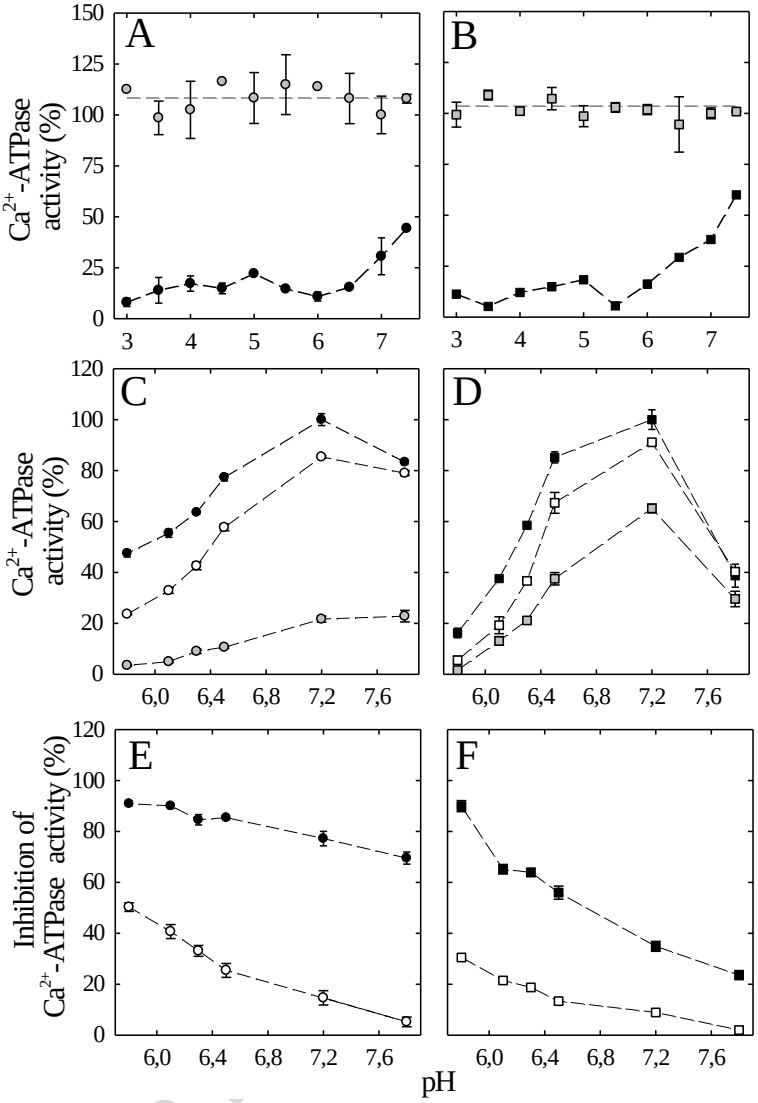

Figure 5. Effect of pH on aluminum inhibition of PMCA and SERCA. Solutions of 40 µM $AlCl_3$ were made at different pH values and then added to the pre-incubation medium (pH 7.2, 25ºC) containing PMCA (**A**) or SERCA (**B**) **(**black symbols). Ca^{2+}-ATPase reaction also was determined at pH 7.2. Solutions with the same pH but in the absence of $AlCl_3$ were used to rule out a pH effect on the pumps (gray symbols). **C** and **D**: Ca^{2+}-ATPase activity was measured in the absence (black symbols) or in the presence of 10 µM (open symbols) or 25 µM (grey symbols) $AlCl_3$ at different pH values for PMCA (C) and SERCA (D). The percentage of aluminum inhibition for PMCA (**E**) and SERCA (**F**) was calculated from the ratio between Ca^{2+}-ATPase activity with and without $AlCl_3$ at each pH value. Results correspond to average ± SD of two independent experiments.

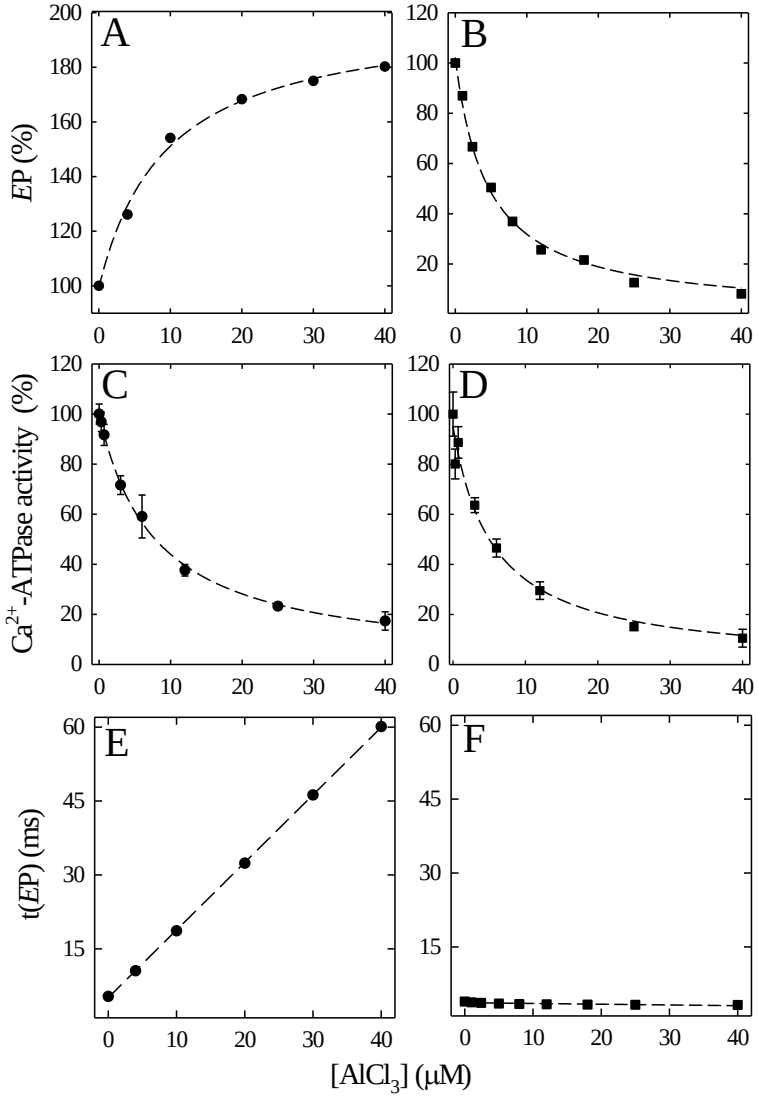

Figure 6: Effect of $AlCl_3$ on phosphorylated intermediate (*E*P). (**A**) and (**B)** shows *E*P as a function of $AlCl_3$ concentration in PMCA and SERCA, respectively. In both, *E*P obtained in the absence of $AlCl_3$ was defined as 100%. In A, dotted line represents the fitting of Eq. 5 to the experimental data obtained for PMCA. In B, dotted line represents the fitting of Eq. 6 to data obtained for SERCA. (**C** and **D**) Ca^{2+}-ATPase activity of PMCA (C) and SERCA (D) in the same conditions in which *E*P was determined (30 μM ATP, see Experimental procedures for details). For both pumps, Ca^{2+}-ATPase activity in the absence of $AlCl_3$ was defined as 100%. Dotted lines on C and D represent the fitting of Eq. 5 to the experimental data. Values of t(*E*P) obtained for PMCA and SERCA are plotted as a function of $AlCl_3$ concentration in **E** and **F**, respectively. Results are representative of two independent experiments.

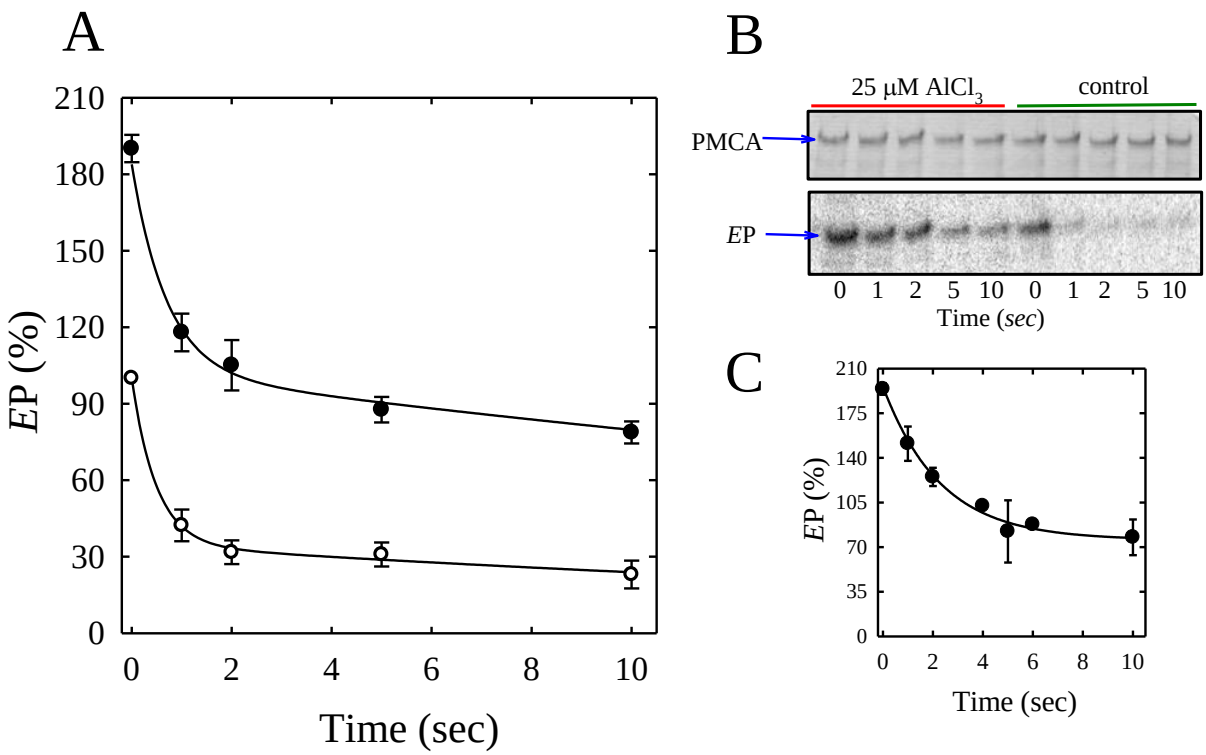

FIGURE 7: Time courses of dephosphorylation of PMCA. **(A)** Phosphorylation of PMCA was carried out at 4°C in the absence (control, empty symbols) or presence of 25 μM $AlCl_3$ (filled symbols). After 3 min incubation, the reaction was stopped by adding a 1 mM ADP solution. Dephosphorylation was allowed to proceed during the time period detailed in each figure and then stopped by protein precipitation with TCA (7%). Results are plotted as the percent of the value in the absence of $AlCl_3$ at zero time of dephosphorylation and these correspond to mean ± SE of 5 independent experiments. Continuous lines represent the fitting of Eq. 7 to the experimental data and parameters obtained are shown in Table 1. **(B)** SDS-PAGE (up) and *E*P autoradiography (down) of a representative experiment included in (A). **(C)** As in (A) the pump was phosphorylated in the presence of 25 μM $AlCl_3$ but the phosphorylation reaction was stopped by adding 0.5 mM ATP solution. Results are plotted as the percent of the value in the absence of $AlCl_3$ at zero time of dephosphorylation and these correspond to mean ± SE of 6 independent experiments. Continuous lines represent the fitting of Eq. 7 to the experimental data and best fitting parameters are shown in Table 1.

Graphical abstract

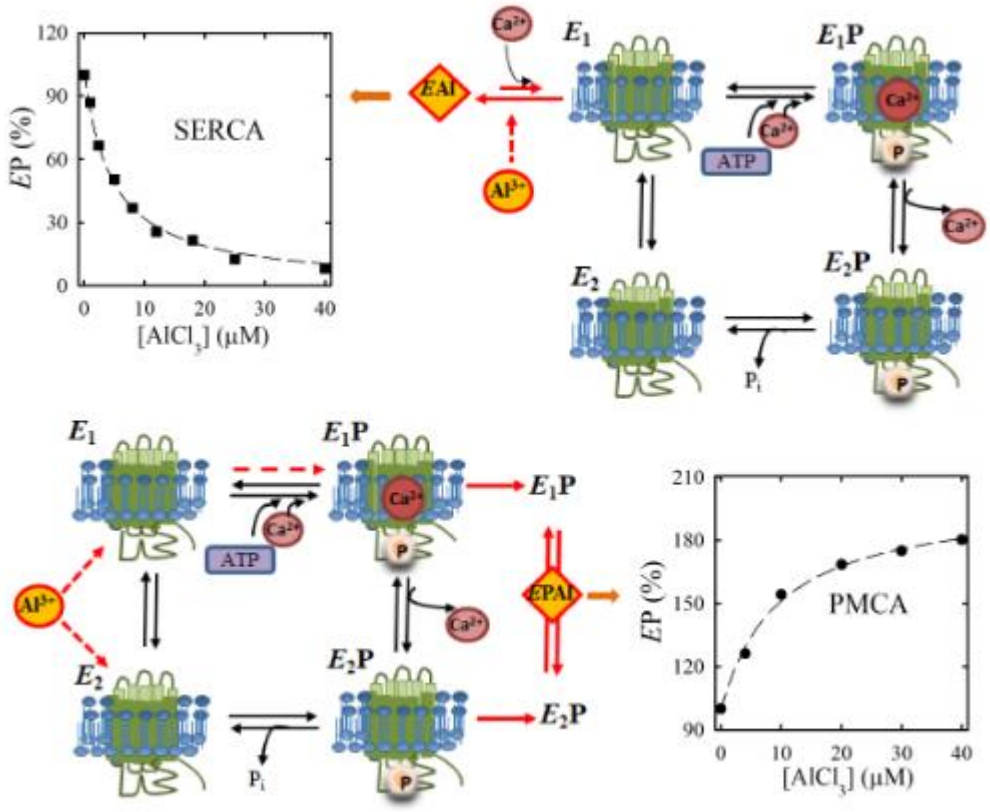

Highlights

(1) Al^{3+} can bind quickly and strongly to PMCA and SERCA
(2) In SERCA, the binding of Al^{3+} is affected by calcium but not in PMCA
(3) In SERCA, Al^{3+} prevents the phosphorylation, while in PMCA it prevents the dephosphorylation of the pump
(4) In PMCA, Al^{3+} fixes the pump in a very stable complex composed mainly by the conformer *E*2P.